

Zeus: Mission to Jupiter

Johnathan Clouse*

University of Colorado, Boulder, CO, 80309-0429, USA

*Graduate Student, Aerospace Engineering Sciences, 1111 Engineering Drive, Boulder, CO, 80309-0429

Contents

I	Introduction	3
II	Preliminary Trajectory Design	4
III	STK Simulation	6
IV	Earth Access	6
V	Europa Injection	6
VI	System Model	6
VII	Conclusion	7

I. Introduction

Jupiter is the largest planet in the solar system, and the closest gas giant to the sun.

A VEEJ (Venus-Earth-Earth-Jupiter) trajectory was considered for launch in 2020. The requirements are outlined as follows:

The sailcraft's actuator was a gimbaled control boom between the sail subsystem and the spacecraft bus, which contained the majority of the spacecraft mass. With the center of mass between the thrust point and the sun, expected disturbances would cause oscillation about some angle between the sun and the axis normal to the sail, α , for a locked gimbal. Changing the gimbal angle, δ , would dampen this oscillation with the right control law. Roll and pitch angles were held to zero for this analysis. Sun sensors determined spacecraft yaw, and had a maximum error of $\pm 0.05^\circ$.

The state-space model had four states: the sun angle (α), the rate of the sun angle ($\dot{\alpha}$), the gimbal angle (δ), and the gimbal angle rate ($\dot{\delta}$). These states were chosen due to their coupling and resulting output (sun angle), as well as being the only dynamic parameters, as seen in Equations 1 and 2. The sail and boom were modeled as rigid bodies, justified by the slow actuation of the gimbal throughout the flight. The sail was modeled as a thin plate, rather than a billowed sail. The state-space model was obtained in a similar manner to that presented by Wie.¹ The equations of motion for a gimbaled thrust vector were obtained for the yaw axis.

System performance was judged by the response to errors, namely a step from $\alpha=0^\circ$ to $\alpha=35^\circ$. Mitigation of disturbance torques was also examined.

II. Preliminary Trajectory Design

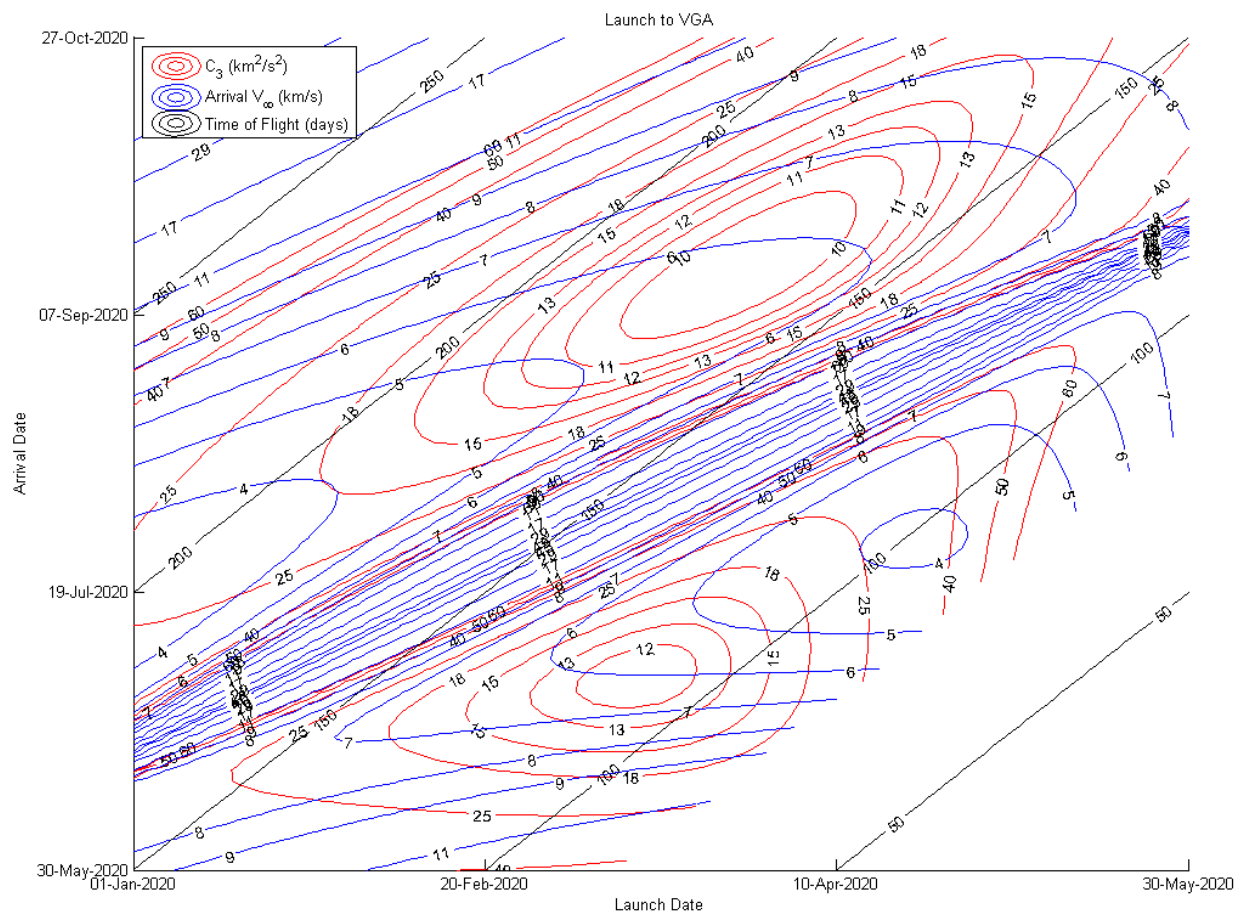


Figure 1. Launch to VGA.

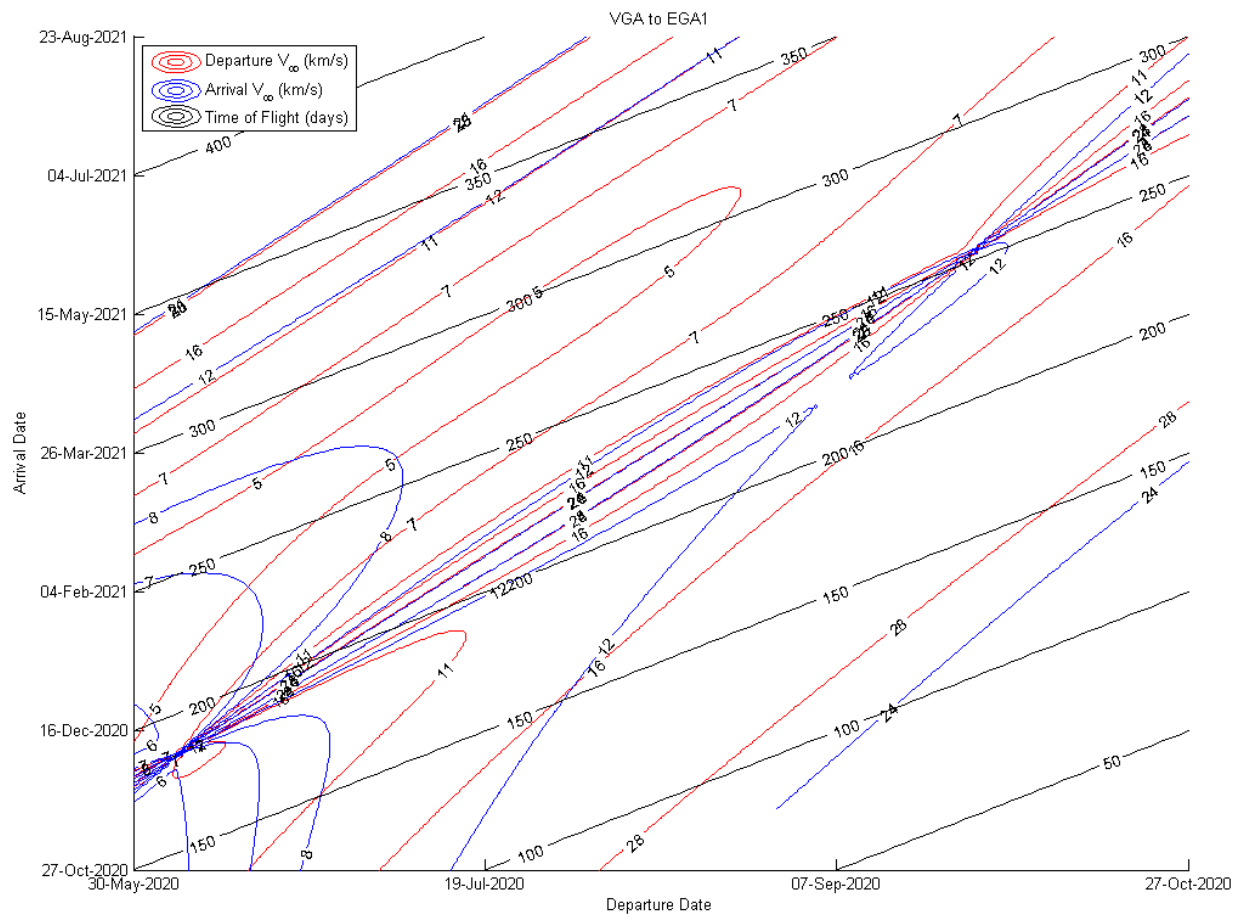


Figure 2. VGA to EGA1.

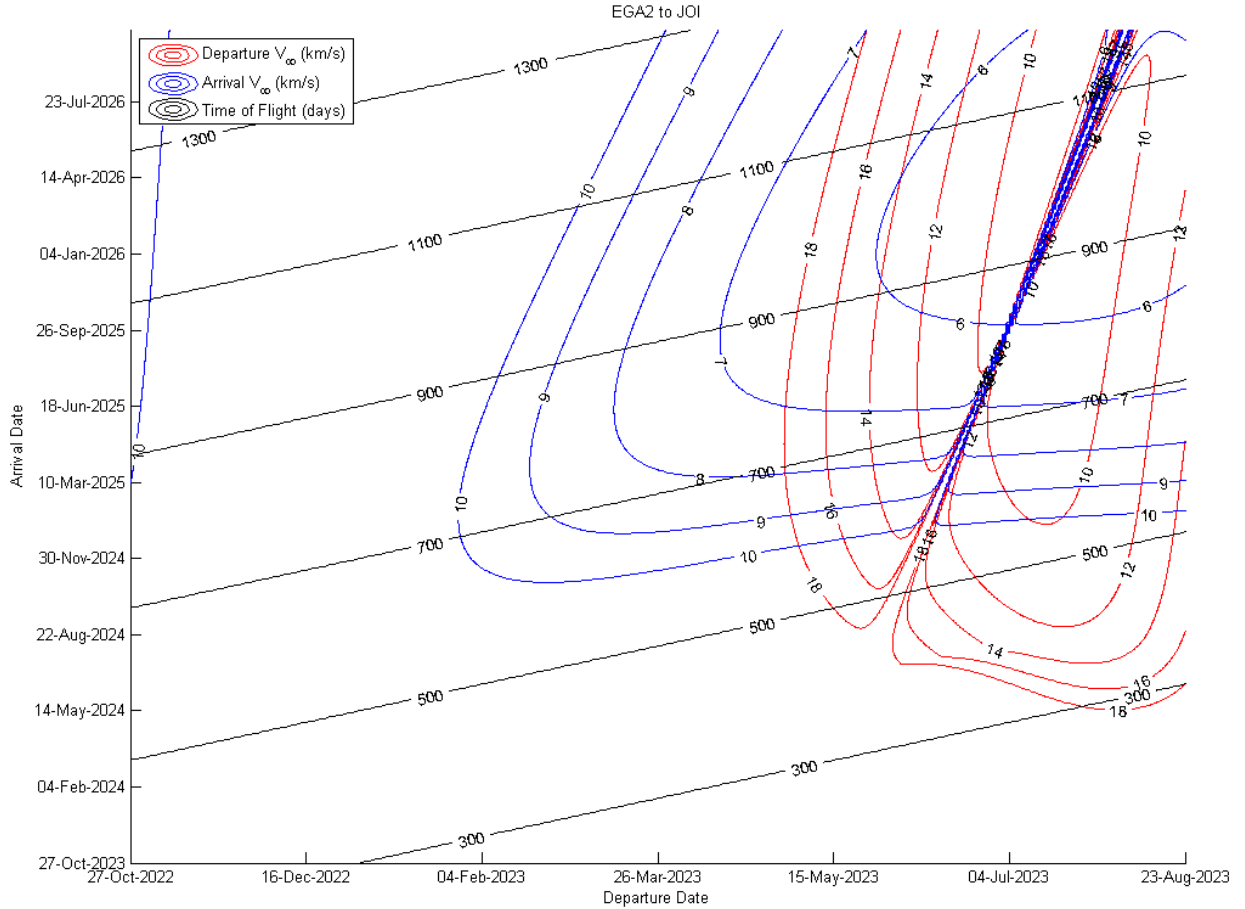


Figure 3. EGA2 to JOI.

Porkchop plots serve as great visual guides to determine low-cost trajectories. However, chaining together multiple gravity assists leads to many potential solutions whose benefits become difficult to compare using several porkchop plots. An algorithm was developed to trim the search space of the possible trajectories, as well as to determine the merits of each trajectory. The algorithm took a predetermined set of windows and determined the lambert solution between the launch, gravity assists, and orbit insertion. Next, launch C_3 and final V_∞ were applied to the initial and final windows to rid the search space of known unusable trajectories. The ΔV difference between planetary encounters on a given date were subsequently calculated; any ΔV difference outside of a tuned tolerance were thrown out. The result was a set of dates

III. STK Simulation

IV. Earth Access

V. Europa Injection

VI. System Model

The equations of motion were linearized about the state $\alpha = \dot{\alpha} = \delta = \dot{\delta} = 0$. Such a state was chosen because it is in equilibrium, due to the force resulting from the solar radiation pressure acting through the sailcraft's center of mass. The system is also stable about this point, as any disturbance to α would cause

oscillation about $\alpha = 0$ for a locked gimbal. The linearized equations are shown below:¹

$$[J_s + (m_s m_p / m) b(b + l)] \ddot{\alpha} + (m_s m_p / m) b l \ddot{\delta} = -(m_p / m) b F_t - T_g + T_{ext} \quad (1)$$

$$[J_p + (m_s m_p / m) l(b + l)] \ddot{\alpha} + [J_p + (m_s m_p / m) l^2] \ddot{\delta} = -(m_p / m) l F_t + (m_p / m) l F_n \delta + T_g \quad (2)$$

VII. Conclusion

The non-optimal controller was able to meet the design criteria without observer errors. However, it proved to not be as robust to such errors as the LQR controller. This is due to the control effort used in both controllers. The LQR design assigned a cost to control effort, so less was used. On the other hand, the non-optimal controller, which was tuned with SISO methods, was otherwise sufficient in meeting control objectives. Perhaps with sensor filtering, observer error could be reduced such that the control effort would also be reduced.

The Luenberger observer was able to reconstruct the entire state from only knowing the sun angle. The poles also drove initial (realistic) initial observer error to zero without forcing the actuator to violate its constraints.

The state feedback mitigated control of the disturbance. Without the integral term, the steady-state error would be untenable for a sailcraft to get the expected thrust. The feedback on the rest of the state ensured a quick rise that did not exceed the defined overshoot limit.

The control methods presented were able to meet the design criteria for single-axis control of the specified solar-sail spacecraft. Further research should be done for both 2-axis gimbaling and combining a gimbal with sail vanes at the edges of the sail, as well as craft with more massive busses and perhaps a gimbaled payload on the other side of the sail. With such research, design flexibility will allow viable missions with reduced time or resource cost.

References

¹Wie, B., "Solar Sail Attitude Control and Dynamics, Part 2," *Journal of Guidance, Control, and Dynamics*, Vol. 27, 2004, pp. 536–544.